Core Expansion, Ruffling, and Doming Effects on Metalloporphyrin Vibrational Frequencies

Kristine Prendergast and Thomas G. Spiro*

Contribution from the Department of Chemistry, Princeton University, Princeton, New Jersey 08544. *Received August 15, 1991*

Abstract: The responsiveness of metalloporphyrin skeletal mode vibrational frequencies to changes in the core size and in the planarity of the macrocycle have been investigated, using normal mode analysis with the recently developed empirical force field for NiOEP (nickel octaethylporphyrin) and NiTPP (*meso*-tetraphenylporphyrin). Crystallographic data for OEP and TPP show correlations of structure parameters with core size: as the core expands, so do the $C_\alpha C_m$ bridge bonds, the pyrrole $C_\alpha C_\beta$ and $C_\beta C_\beta$ bonds, and the $C_\alpha C_m C_\alpha$ bridge angles, while the $C_\alpha N$ bonds contract. These empirical correlations were used to define a structural model of core expansion in order to calculate the vibrational frequency dependence. The kinematic consequences of core expansion are negligible, but when the bond stretching force constants were scaled to the bond distances, using the empirical equation of Burgi and Dunitz, the frequency correlations were calculated nearly quantitatively. Core size effects were also examined with QCFF/Pi semiempirical calculations on a metallo-OEP model at a series of metal–nitrogen distances. The trends in geometry were in reasonable agreement with the crystallographic data except that $C_\beta C_\beta$ was calculated to decrease strongly with core size, contrary to the observed trend. Consequently, the calculated frequency dependencies had slopes differing in sign from the observed slopes for modes having major $C_\beta C_\beta$ contributions, ν_3 and ν_{11}. The kinematics of porphyrin ruffling and doming were calculated to produce appreciable downshifts in the ν_{10} and ν_{19} modes, involving out-of-phase stretching of the $C_\alpha C_m$ bridge bonds, due to out-of-plane displacements of the C_m atoms. MNDO/3 calculations, carried out on zinc(II) porphine with dihedral angles artificially constrained to produce ruffled and domed structures, showed the ring bond distances to be essentially unaffected by the out-of-plane distortions. Consequently, the changes in frequency should be calculable from kinematics alone if the distortion is imposed externally, e.g. by crystal packing or by steric forces in proteins. Some ruffled or domed metalloporphyrins show additional deviations from expectations based on core size, however, probably because of electronic influences. Thus, the ruffled form of NiOEP shows downshifts of ν_2 and ν_{11}, relative to the planar form, which are calculable by bond distance scaling, since the $C_\beta C_\beta$ distance is observed to lengthen. Five-coordinate complexes of Fe(II), Co(II), and Mn(II) show depressed ν_4 frequencies; this effect is suggested to arise from interaction of the d_{z^2} electrons with the filled a_{2u} π orbitals, an interaction permitted in these C_{4v} complexes, and which is made effective by the low valency of the metal ions.

Introduction

Because of the continuing interest in metalloporphyrin structure and reactivity, particularly in connection with the investigation of heme proteins and of photoreaction centers, vibrational spectra of metalloporphyrins have been studied extensively.[1] The high symmetry of the porphyrin ring and the mode selectivity available with variable wavelength resonance Raman spectroscopy, as well as the extensive use of isotopic substitution, have made possible detailed and reliable vibrational assignments. A general valence force field has recently been developed, which gives a satisfactory account of essentially all of the modes of the nickel complexes of porphine, tetraphenylporphyrin (TPP),[2] and octaethylporphyrin (OEP).[3]

With the modes accurately calculable, it is now possible to analyze the physical basis for the structural sensitivities of porphyrin vibrational frequencies, which have been noted empirically. The most striking of these sensitivities is associated with the porphyrin core size.[4] All of the skeletal mode frequencies above 1450 cm^{-1} show a negative linear dependence on the core size, defined as the distance between the center of the porphyrin ring and the pyrrole nitrogen atoms, when this relationship is examined for metal complexes of TPP,[5] OEP,[6] and protoporphyrin.[5,7] Because the core size is responsive to the spin and ligation states of the central metal ion,[8] the core size relations play a key role in the analysis of heme protein RR spectra. The sensitivity to core size has been thought to reside in the porphyrin–methine bridges.[7,9] If the pyrrole rings are viewed as rigid structural elements, then expansion of the porphyrin ring must involve stretching of the bridge bonds and/or opening up of the bridge angles. Consequently, the frequencies associated with the bridge bonds are expected to decrease. Indeed, the slopes of the core size correlations have been found to show a rough correlation with the percentage contribution of $C_\alpha C_m$ stretching to the modes.[7] Shelnutt and co-workers,[10a] noting that core size plots seem to have different slopes for octaalkylporphyrins than for the sterically hindered octaalkyltetraphenylporphyrins, found a more consistent correlation with the pyrrole $C_\alpha NC_\alpha$ angle. Beyond these observations, the core size correlations have not been evaluated critically with regard to the mechanism.

In this study, we examine the dependence of structural parameters and vibrational frequencies on core size, using data for a wide range of metal complexes of OEP and TPP. Although the $C_\alpha C_m$ bond length and $C_\alpha C_m C_\alpha$ angle do indeed increase with increasing core size, we find that the structural parameters within the pyrrole ring are not invariant; the $C_\alpha C_\beta$ and $C_\beta C_\beta$ bonds also lengthen, while the $C_\alpha N$ bonds shorten as the core size increases. Taking these trends into account, we find that the observed core size correlations of the mode frequencies can be calculated with reasonable accuracy if the porphyrin force field is adjusted by scaling the bond stretching force constants to the bond distance, using the equation advocated by Burgi and Dunitz.[11] Thus, the

* Author to whom correspondence should be addressed.

(1) Spiro, T. G.; Li, X. Y. In *Biological Applications of Raman Spectroscopy*; Spiro, T. G., Ed.; Wiley-Interscience: New York, 1988; Vol. III, Chapter 1.
(2) Li, X. Y.; Czernuszewicz, R. C.; Kincaid, J. R.; Su, Y. O.; Spiro, T. G. *J. Phys. Chem.* **1990**, *94*, 31.
(3) Li, X. Y.; Czernuszewicz, R. S.; Kincaid, J. R.; Stein, P.; Spiro, T. G. *J. Phys. Chem.* **1990**, *94*, 47.
(4) Spaulding, L. D.; Chang, C. C.; Yu, N.-T.; Felton, R. H. *J. Am. Chem. Soc.* **1975**, *97*, 2517.
(5) Parthasarati, N.; Hansen, C.; Yamaguchi, S.; Spiro, T. G. *J. Am. Chem. Soc.* **1987**, *109*, 3865.
(6) Oertling, W. A.; Salehi, A.; Chung, Y. C.; Leroi, G. E.; Chang, C. K.; Babcock, G. T. *J. Phys. Chem.* **1987**, *91*, 5587.
(7) Choi, S.; Spiro, T. G.; Langry, K. C.; Smith, K. M.; Budd, L. D.; LaMar, G. N. *J. Am. Chem. Soc.* **1982**, *104*, 4345.
(8) Spiro, T. G. In *Iron Porphyrins*; Lever, A. B. P., Gray, H. B., Eds.; Addison-Wesley: Reading, MA, 1983; Vol. 2, p 91.
(9) Warshel, A. *Annu. Rev. Biophys. Bioeng.* **1977**, *6*, 273.
(10) (a) Shelnutt, J. A.; Medforth, C. J.; Berber, M. D.; Barkigia, K. M.; Smith, K. M. *J. Am. Chem. Soc.* **1991**, *113*, 4077–4087. (b) Alden, R. G.; Crawford, B. A.; Dooley, R.; Ondrias, M. R.; Shelnutt, J. A. *J. Am. Chem. Soc.* **1989**, *111*, 2070.
(11) Burgi, H.; Dunitz, J. D. *J. Am. Chem. Soc.* **1987**, *109*, 2924.

0002-7863/92/1514-3793$03.00/0

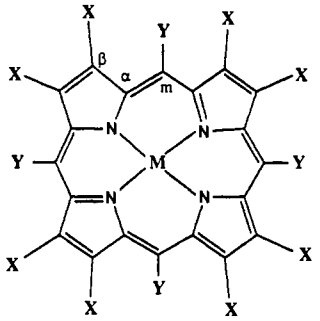

Figure 1. Structure of a generic porphyrin, with atom labeling scheme. For OEP, X = ethyl and Y = H, and for TPP, X = H and Y = phenyl.

physical basis for the experimental correlations resides in the adjustments of all of the bonds in the macrocycles to the consequences of altering the size of the core. We also examined the core size effect via QCFF/Pi[12] calculations, in order to determine the extent to which the observed structural variations are encompassed by a semiempirical treatment of the porphyrin electronic structure. The method does reasonably well for all bond lengths except $C_\beta C_\beta$, which is predicted to decrease with core expansion, whereas the $C_\beta C_\beta$ lengths actually increase.

Deviations from the core size/frequency correlations have been noted for a number of metalloporphyrins,[5,13] and explanations have been sought in electronic effects or in distortions from the planar porphyrin geometry.[3,14] Doming and ruffling distortions,[15] produced by tilting or swivelling of the pyrrole rings, have drawn particular attention, since these distortions are frequently seen in heme proteins. We have determined that the altered kinematic interactions produced by these distortions should have noticeable effects on the vibrational frequencies, particularly for the ν_{10} and ν_{19} modes, which involve out-of-phase stretching of the $C_\alpha C_m$ bridge bonds. The actual situation in domed and ruffled metalloporphyrins is more complex than predicted by kinematics, probably because the electronic properties of the metal ion that lead to the distortion also have other influences on the mode frequencies. For example, five-coordinate high-spin complexes of Fe(II), Co(II), and Mn(II), for which there is crystallographic evidence of doming,[16] show frequency depressions for ν_4,[5] and this can be attributed to an electronic interaction of the d_{z^2} electrons with the filled porphyrin a_{2u} π orbital. In the ruffled form of NiOEP, frequency lowerings are seen for the $C_\beta C_\beta$ stretching modes ν_2 and ν_{11},[10b,13] which can be attributed to the observed lengthening of the $C_\beta C_\beta$ bonds in the ruffled crystal structure.[17] This effect may be a peculiarity of Ni(II), however, since lengthened $C_\beta C_\beta$ bonds are not seen for all ruffled metalloporphyrins, but only those having particularly small metal ions. We have carried out MNDO/3 calculations[18,19] on zinc(II) porphine which was artificially constrained to adopt domed or ruffled conformations. The calculated changes in the bond distances were negligible. Consequently, it seems likely that if out-of-plane distortions are imposed by external forces, e.g. crystal packing or protein nonbonded forces, then the effects on the vibrational frequencies should be those expected on kinematic grounds.

Results and Discussion

A. Core Size. Spaulding et al.[4] discovered that the frequency of an anomalously polarized RR band of metalloporphyrins, later assigned as the A_{2g} $C_\alpha C_m$ stretching mode ν_{19},[20] was negatively correlated with the porphyrin core size. Similar correlations were then found for other bands,[21,22] and Choi et al.,[7] in a study of iron protoporphyrin complexes that model heme proteins, reported negative correlations with core size for *all* the skeletal modes above 1450 cm^{-1}. These correlations have since been refined and have been extended to TPP's[5] and OEP's,[6] to chlorins,[23] and to isobacteriochlorins.[24] Thus, the tendency for skeletal mode frequency to decrease with increasing core size is a very general one for porphyrins and hydroporphyrins.

Table I. Molecules Used in Generating the Crystallographic Data Base

compound	core size, Å	distortion[a]	ref
NiOEP	1.929	ruffled	17
NiOEP	1.958	planar	26
$FeOEP(NO)ClO_4$	1.973	M OOP	31
$CoOEP(3Pic)_2$	1.992	planar	32
$FeOEP(3ClPy)_2ClO_4$	2.006	ruffled	31
$FeOEP(2MeIm)^+$	2.008	M OOP	33
VOEP(O)	2.031	domed	34
FeOEP(Py)(NCS)	2.034	domed	35
$SnOEP(Cl)_2$	2.082	planar	36
TlOEPCl	2.100	domed	37
CoTPP	1.949	ruffled	38
FeTPP	1.972	ruffled	39
CoTPP(1MeIm)	1.973	planar	40
$CoTPP(Pip)_2NO_3$	1.979	planar	41
$CoTPP(Pip)_2$	1.987	planar	42
FeTPP(Py)(NCS)	1.988	ruffled	35
$FeTPP(Im)_2Cl$	1.989	ruffled	43
MnTPP(Cl)	1.990	domed	44
$FeTPP(NO)(H_2O)ClO_4$	1.999	planar	31
$FeTPP(Py)_2$	2.001	planar	45
$FeTPP(Pip)_2$	2.004	planar	46
(FeTPP)2O	2.027	domed	47
ZnTPP	2.036	planar	48
FeTPP(2MeIm)	2.044	domed	49
$SnTPP(Cl)_2$	2.098	planar	50

[a] M OOP, metal above the porphyrin ring, which is roughly planar; domed, porphyrin cupped, with atoms in descending planes M, N, C_α, C_m, C_β; ruffled, methine bridges alternate up and down, pyrrole nitrogens coplanar.

Soon after the discovery of Spaulding et al., Warshel[9] proposed that the core size effect is due to strain on the methine bridges (see Figure 1 for a structural diagram) when the rigid pyrrole rings are forced outward by expansion of the central metal ion. Results of a QCFF/Pi calculation on porphine were reported,[9] which gave qualitative support to this concept. Subsequently, Choi et al.[7] noted that the modes which showed the highest core-size sensitivity did have large contributions from $C_\alpha C_m$ stretching, as determined by the normal coordinate analysis of Kitagawa and co-workers,[20] although the correlation of the core-size slopes with the $C_\alpha C_m$ potential energy contribution was far from exact. It should be possible to investigate the effect more quantitatively by adjusting the porphyrin force field to the core size using an appropriate model. This is what we set out to do in the present study.

A general valence force field (GVFF) has recently been developed by Li et al.[2,3] which calculates essentially all the modes of the Ni(II) complexes of porphine, OEP, and TPP and several isotopomers, with only slight alteration of the force constants to allow for electronic effects of the different substituents. Moreover, the bond stretching force constants correlate with bond distance in good agreement with the empirical equation advanced by Burgi and Dunitz,[11] as discussed by Li et al.[2,3] Accordingly, we decided to apply the NiOEP and NiTPP force fields to a geometric model

(12) Warshel, A.; Lappicirella, A. *J. Am. Chem. Soc.* **1981**, *103*, 4664.
(13) Czernuszewicz, R. S.; Li, X. Y.; Spiro, T. G. *J. Am. Chem. Soc.* **1989**, *111*, 7024.
(14) Sarma, Y. A. *Spectrochim. Acta* **1989**, *45A*, 649.
(15) Hoard, J. L. *Ann. N.Y. Acad. Sci.* **1973**, *206*, 18.
(16) Scheidt, W. R.; Lee, Y. J. *Struct. Bonding* **1987**, *64*, 2.
(17) Meyer, E. F., Jr. *Acta Crystallogr.* **1972**, *B28*, 2162.
(18) Dewar, M. S.; Zoebisch, E. G.; Healy, E. T.; Stewart, J. J. P. *J. Am. Chem. Soc.* **1985**, *107*, 3902.
(19) Liotard, D. A.; Healy, E. F.; Ruiz, E. F.; Dewar, M. S. *QCPE* **1989**, *506*, Version 2.1.
(20) Kitagawa, T.; Abe, M.; Ogoshi, H. *J. Chem. Phys.* **1978**, *69*, 4526.
(21) Huong, P. V.; Pommier, J. C. *C. R. Acad. Sci. Ser. C* **1977**, *285*, 519.
(22) Spiro, T. G.; Stong, J. D.; Stein, P. *J. Am. Chem. Soc.* **1979**, *101*, 2648.
(23) Ozaki, Y.; Iryiama, K.; Ogoshi, H.; Ochiai, T.; Kitagawa, T. *J. Phys. Chem.* **1986**, *90*, 6105.
(24) (a) Melamed, D.; Sullivan, E.; Prendergast, K.; Strauss, S.; Spiro, T. G. *Inorg. Chem.* **1991**, *30*, 1308. (b) Mylrajan, M.; Andersson, L. A.; Loehr, T. M.; Sullivan, E. P.; Strauss, S. H. Submitted for publication.

Table II. Best Fit Lines[a] for Internal Coordinate versus Core Size Plots in Figure 2

coordinate	*A*	*B*	*R*[b]
$C_\alpha C_m$	1.118	+0.131	0.561
$C_\alpha C_\beta$	1.384	+0.030	0.211
NC_α	1.526	−0.073	0.224
$C_\beta C_\beta$	1.096	+0.127	0.516
$C_\alpha C_m C_\alpha$	63.8	+31.2	0.618
$C_\alpha C_m$	1.078	+0.157	0.869
$C_\alpha C_\beta$	1.281	+0.080	0.467
NC_α	1.606	−0.111	0.744
$C_\beta C_\beta$	1.026	+0.163	0.381
$C_\alpha C_m C_\alpha$	76.3	+23.6	0.891

[a] $y = A + Bx$; y = coordinate, x = core size; units are Å, except $C_\alpha C_m C_\alpha$ for which y and a are degrees and b is degrees/Å. [b] R = correlation coefficient.

of core size expansion, using the Burgi and Dunitz equation for force constant scaling. Our *initial* model was based on Warshel's concept of methine bridge strain: the pyrrole rings were held at fixed geometry and allowed to move outward along the metal–pyrrole bonds. The increasing distance between pyrroles was accommodated by lengthening the $C_\alpha C_m$ bonds and expanding the $C_\alpha C_m C_\alpha$ angles. When the normal modes were calculated as a function of increasing core size, those having dominant $C_\alpha C_m$ contributions did indeed show decreasing frequency, but the slopes were in only modest agreement with experiment, and modes having dominant $C_\beta C_\beta$ contributions were nearly invariant, although the experimental data show negative correlations for these modes as well. These discrepancies prompted us to reexamine the geometric model of core size expansion in the light of the available crystallographic data.

1. Structural Data and the Geometric Model. Table I lists 10 OEP and 15 TPP complexes for which X-ray crystal structures have been reported. They cover a wide range of core sizes, from 1.93 to 2.10 Å. About half of the structures have planar porphyrin rings, the rest showing varying degrees of ruffling (propeller twist of the pyrroles) or doming (tilting of the pyrroles toward one side of the plane). Two examples, listed as MOOP, have essentially planar porphyrins with the metal ion out of the plane. For planar and ruffled examples, the core size coincides with the metal–pyrrole bond distance, while for domed and MOOP examples, the core size (defined as the distance from the pyrrole N atoms to C_t, the projection of the metal ion onto the N_4 plane) is somewhat smaller than the bond distance.

In Figure 2, we plot the four skeletal bond distances, $C_\alpha C_m$, $C_\alpha C_\beta$, $C_\alpha N$, and $C_\beta C_\beta$, as well as the $C_\alpha C_m C_\alpha$ angle as a function of the core size for the compounds in Table I. These five internal coordinates are sufficient to define the geometry of a planar porphyrin at a given core size, assuming 4-fold symmetry. For those compounds having less than 4-fold crystallographic symmetry, the internal coordinates were averaged. The $C_\alpha C_m$ distance and $C_\alpha C_m C_\alpha$ angle show strong positive correlations, as expected, although the OEP and TPP data fall on separate lines. At a given core size, the $C_\alpha C_m$ bond is about 0.01 Å longer and the $C_\alpha C_m C_\alpha$ angle is about 2° smaller for TPP than for OEP, presumably reflecting the inductive effect of the meso-phenyl substituents. For the remaining three distances, which define the pyrrole rings, the data are more scattered, but it is evident that the assumption of an invariant pyrrole geometry is not valid. The $C_\alpha N$ distances decrease with increasing core size, while the $C_\alpha C_\beta$ and $C_\beta C_\beta$ distances increase. The scale of these variations is not qualitatively different than for the $C_\alpha C_m$ variation. Thus, the picture that emerges from the crystallographic data is that core expansion leads to $C_\alpha N$ *contraction* as well as expansion of all the outer ring bonds, $C_\alpha C_m$, $C_\alpha C_\beta$, and $C_\beta C_\beta$.

The solid lines in Figure 2 represent least-squares fits to the data, determined separately for the OEP's and TPP's. We examined the data for ruffled and domed porphyrins separately (open symbols in the figure), since it might be expected (see below) that these distortions affect the bond distances and angles. Although ruffled and domed complexes produce outlying points in some of the plots, their overall scatter is not sufficiently greater than that of the planar porphyrins to justify deleting them from the least-squares fits. Table II gives the slopes and intercepts, as well as the correlation coefficients, for the least-squares lines. Together, these constitute our empirical model for core size expansion. To check the internal consistency of the model, we used it to calculate core size dependencies for two other structural parameters, the porphyrin center-to-C_m distance, C_tC_m, and the $C_mC_\alpha C_\beta$ angle. These are shown as dot–dashed line in Figure 3, where the experimental data are shown for comparison. The agreement is seen to be satisfactory.

Table III. Molecules Used in Generating the Skeletal Mode Frequency Data Base

compound[a]	core size, Å	distortion[b]	reference porphyrin[c]
NiOEP[3]	1.958	planar	NiOEP[26]
$FeOEP(Im)_2Cl$[57]	1.989	ruffled	$FeTPP(Im)_2Cl$[43]
$FeOEP(Im)_2$[58]	2.004	planar	$FeTPP(Pip)_2$[46]
CoOEP[6]	1.976	ruffled	CoTPP[51]
CuOEP[6]	2.000	ruffled	CuTPP[52]
VOOEP[59]	2.031	domed	VOOEP[34]
ZnOEP[6]	2.036	planar	ZnTPP[48]
$FeOEP(DMSO)_2$[23]	2.045	planar	$FeTPP(TMSO)_2$[53]
$RuOEP(Py)_2$[60]	2.047	planar	$RuOEP(Py)_2$[47]
NiTPP[5]	1.955	planar	NiTPPyP[54]
CoTPP(2MeIm)[5]	1.973	planar	CoTPP(1MeIm)[40]
$FeTPP(Im)_2Cl$[5]	1.989	ruffled	$FeTPP(Im)_2Cl$[43]
MnTPP(Cl)[5]	1.990	ruffled	MnTPP(Cl)[44]
$FeTPP(Im)_2$[5]	1.997	planar	$FeTPP(Pip)_2$[46]
FeTPP(Cl)[5]	2.019	M OOP	FeTPP(Cl)[55]
FeTPP(2MeIm)[5]	2.044	M OOP	FeTPP(2MeIm)[44]
$FeTPP(DMSO)_2$[5]	2.045	planar	$FeTPP(TMSO)_2$[53]
MnTPP(2MeIm)[5]	2.065	saddle	MnTPP(2MeIm)[56]
$SnTPP(Cl)_2$[5]	2.098	planar	$SnTPP(Cl)_2$[50]

[a] Reference notes source of frequency data. [b] M OOP, metal above the porphyrin plane, which is roughly planar; domed, porphyrin cupped, with atoms in descending plane M, N, C_α, C_m, C_β; ruffled, methine bridges alternate up and down, pyrrole nitrogens coplanar; saddle, pyrrole nitrogens NOT coplanar, alternate up and down. [c] Reference porphyrin from which core size was extracted.

2. Skeletal Mode Frequencies. The least-squares lines of Figure 2 were then used to adjust the geometry in calculating normal mode frequencies as a function of core size using the NiOEP[3] and NiTPP[2] force fields.[25] When the force constants were held constant, the skeletal mode frequencies varied less than 3 cm^{-1} over the experimental range of core sizes. Thus, the kinematic effects of the geometry adjustment to core expansion are negligible. Next, the force constants were scaled to the bond distances with the Burgi-Dunitz equation.[11,25] The resulting plots of mode frequency against core size are shown as solid lines in Figures 4 and 5 for TPP and OEP, respectively. Also shown are experimental frequencies from RR spectra for the OEP and TPP complexes listed in Table III, obtained in solution (mostly CH_2Cl_2). All the Raman active skeletal modes above 1430 cm^{-1} and ν_4 are included, except that ν_{28} has not been identified for most complexes. The least-squares fits to these experimental data are shown as dashed lines in Figures 4 and 5. These least-squares lines differ slightly from those reported previously for OEP[6] because of a somewhat larger data set. In cases where the crystal structure is not available,

(25) Calculations were performed on a VAX 11-780. Frequencies were calculated using the idealized TPP and OEP geometries described above, and the NiTPP and NiOEP vibrational force fields.[2,3] The GF matrix method was employed, using the programs GMAT and FPERT for the construction of the G matrix and solution of the vibrational secular equation (Snyder, R. G.; Schachtschneider, J. H. *Spectrochim. Acta* **1965**, *21*, 169). The force constant scaling relationship of Burgi and Dunitz[11] has been used to incorporate the electronic effects of core expansion into the empirical potential, where, k is the stretching force constant and r is the bond length: $k = 10^{-[(r-1.85)/0.55]}$ QCFF/Pi[12] was also used to examine the geometry and frequency variations with core size. Planar NiOEP was used as the structural model; ethyl groups were treated as point masses and a nickel(II) ion was included as a point charge/mass. The core size (Ni–N distance) was calculated at 1.922, 1.968, 1.996, and 2.064 Å by setting the idealized Ni–N bond length parameter to 0.5, 1.0, 1.3, and 2.0 Å, respectively. The remainder of the porphyrin parameters were set at the default values provided by Bocian and co-workers (R. Donohoe, personal communication).

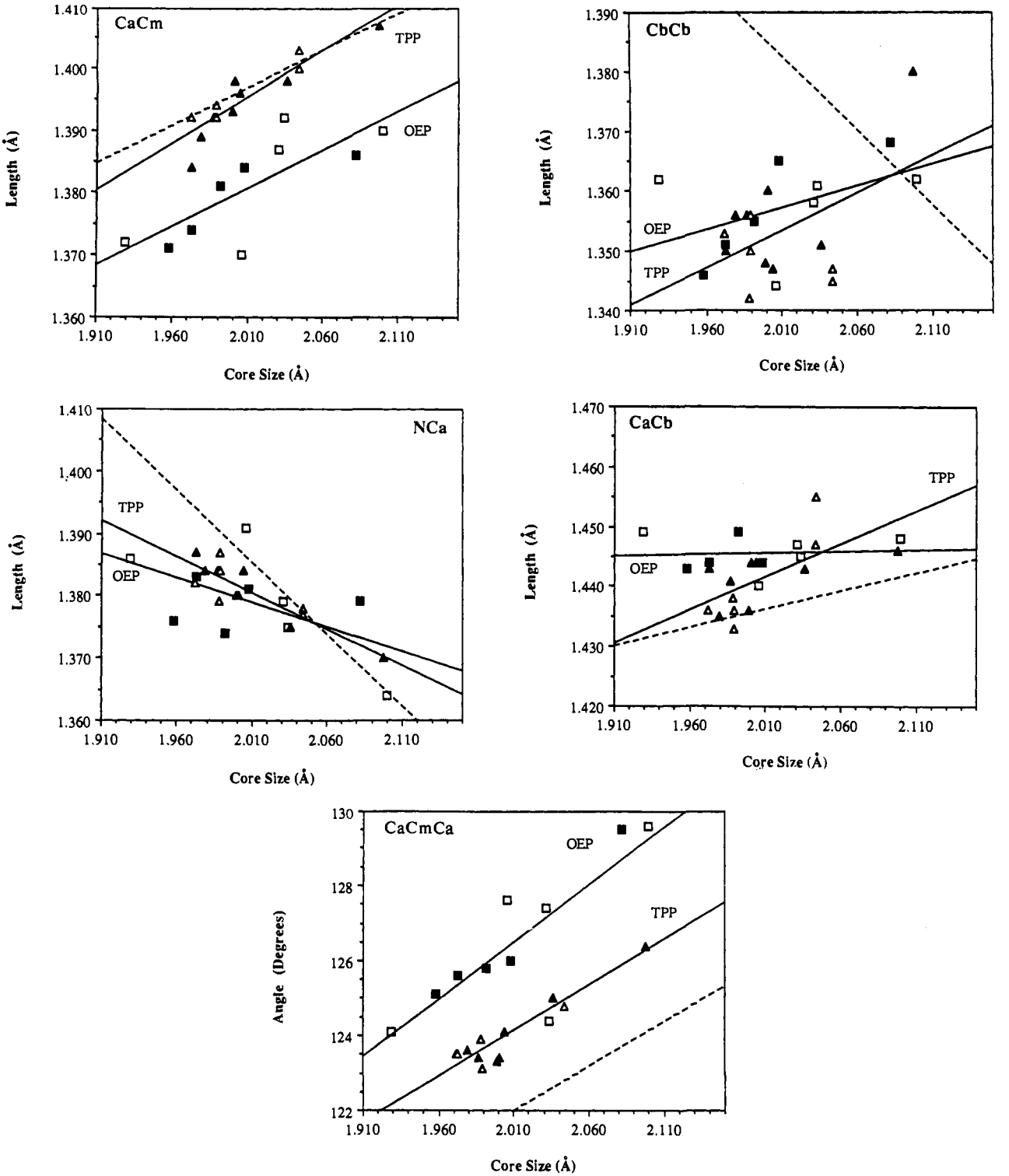

Figure 2. Bond lengths and angles as a function of core size for the OEP's (squares) and TPP's (triangles) listed in Table I. Filled symbols are used for planar porphyrins, while open symbols are used for domed or ruffled porphyrins (see Table I). The solid lines were obtained by linear regression of the data. The dashed lines represent the QCFF/Pi predictions for OEP (point mass ethyls).

core sizes were estimated from crystal structures of closely related species, which are listed in Table III as "reference porphyrin". The axial ligands are the same, or are chemically similar (e.g. piperidine in place of imidazole), but TPP structures are used for several of the OEP complexes, and NiTPyP (tetrapyridylporphyrin) is used for NiTPP. To the extent that porphyrin structures with the same metal and axial ligand can be compared, the substituents seem not to affect the core size significantly. It is reassuring in this regard that the OEP data, plotted with some OEP and some TPP core sizes, show no more scatter than does the TPP data. The structures in Table III also include domed and ruffled as well as MOOP examples. As in Figure 2, the data in Figure 3 are ploted with open symbols for domed and ruffled and solid symbols for planar porphyrins. Again, there is no significant difference in the scatter between the two sets of data. (Individual cases are, however, considered below.)

Indeed, the scatter of the vibrational frequencies is noticeably smaller than the scatter in the bond distances seen in Figure 2. We considered the possibility that the vibrational frequencies might vary more smoothly with core size, because the bond distance variations happen to have compensating effects on the normal mode frequencies. To test this idea we calculated frequencies for

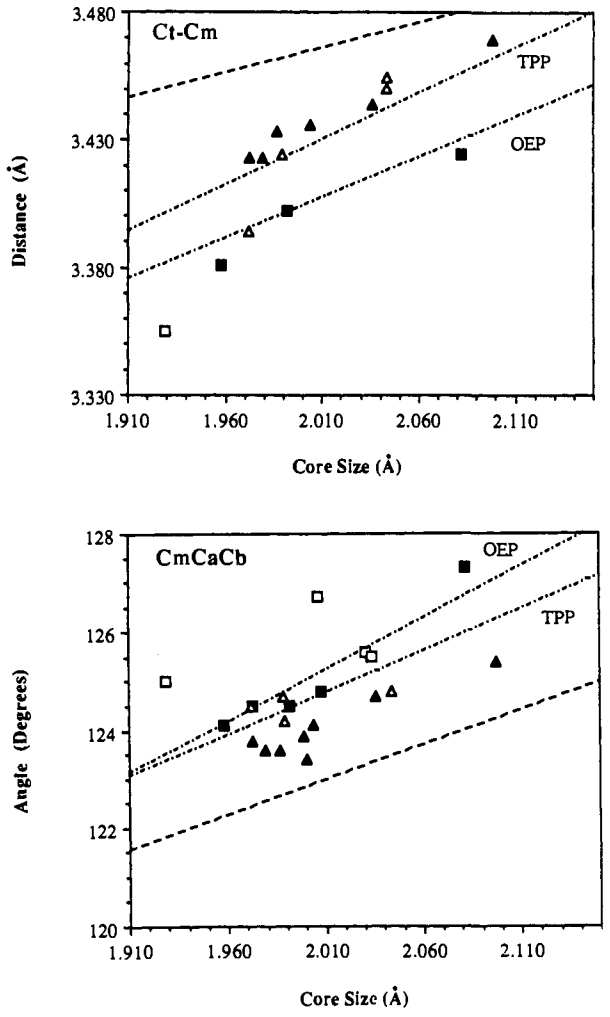

Figure 3. Plots of C_t–C_m and $C_mC_\alpha C_\beta$ against core size. The dot–dash lines are calculated with the geometric model based on the best-fit lines for the five lengths and angles in Table II, while the dashed lines are the QCFF/Pi predictions. Symbols as in Figure 2.

several complexes using bond distance scaling to the actual crystal structures (rather than the least-squares expectation values). The result was to introduce as much scatter into the frequency/core-size plots as is seen among the bond distances, thereby negating the hypothesis. Another possibility is that the scatter in the structural data is due to crystal packing forces being accommodated differently for different porphyrins, and these differences disappear in solution. If this were the case, then one would expect to see appreciable deviations from the core-size plots for vibrational spectra of crystalline samples. Except for NiOEP (see below), discrepancies of this kind have not come to light, although they have not been sought systematically. A third possibility is that the scatter in the crystallographic bond distances simply reflects the inherent accuracy of diffraction analysis for molecules as large as porphyrins, and that for bond distance changes at the level of thousandths of angstroms, the vibrational spectra, although less straightforwardly interpretable, are a more sensitive measure. Indeed, the reported standard deviations for crystallographically determined band distances are frequently in the 0.005–0.015 Å range (see e.g. Table VIII), a range that includes most of the scatter seen in Figure 2. As discussed below, the data on the various crystal forms of NiOEP support this interpretation.

Table IV compares the scaled force field (GVFF) and least-squares (observed) slopes and also indicates the major bond stretching contributors to the modes. The core size dependencies predicted by force constant scaling agree reasonably well with the experimental data. The general decrease in frequency with increasing core size is reproduced by the model, and the ordering of the modes by core size sensitivity is maintained, with one

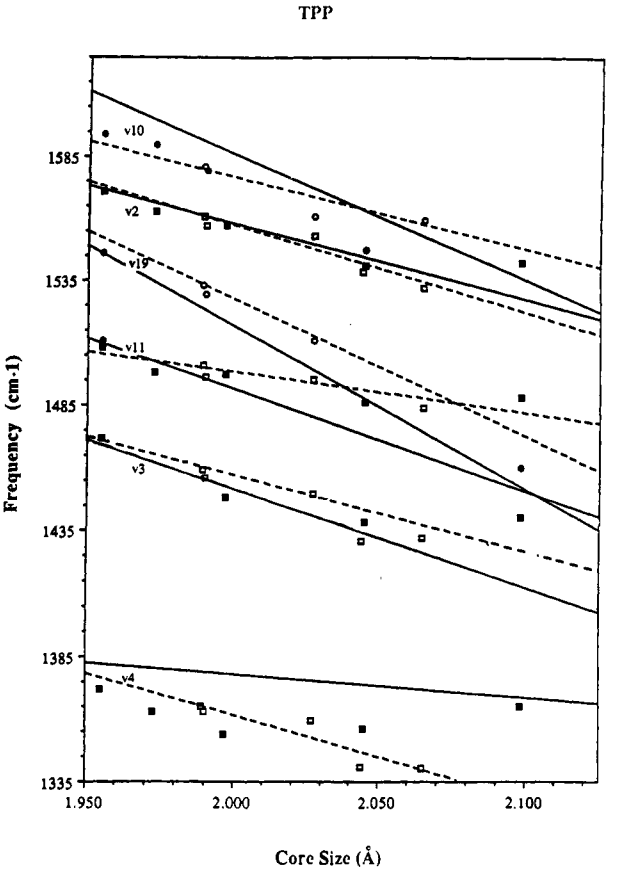

Figure 4. Core size dependence of the TPP skeletal modes predicted from the geometric model via force constant scaling (solid lines) compared with the experimental data (see Table III for listing of complexes included in the plot) and best-fit lines (dashed). Filled symbols are planar porphyrins, and open symbols are domed or ruffled porphyrins. Circles and squares alternate in the order ν_{10}, ν_2, ν_{19}, ν_{11}, ν_3, and ν_4.

Table IV. Comparison of Observed and Calculated Slopes for the Best-Fit Line to the Frequency versus Core Size Plots

OEP

normal mode			slope, cm^{-1}/Å	
label	composition[a]	observed[b]	GVFF[c]	QCFF/PI[d]
ν_{10}	$C_\alpha C_m$	−512	−435	−333
ν_{19}	$C_\alpha C_m$	−455	−418	−346
ν_3	$C_\alpha C_m$, $C_\beta C_\beta$	−453	−236	−88
ν_{11}	$C_\beta C_\beta$	−376	−400	+44
ν_2	$C_\beta C_\beta$, $C_\alpha C_m$	−286	−357	−284
ν_4	NC_α, $C_\alpha C_\beta$	−184	+45	−31

TPP

normal mode			slope, cm^{-1}/Å
label	composition[a]	observed[b]	GVFF[b]
ν_{19}	$C_\alpha C_m$	−543	−650
ν_{10}	$C_\alpha C_m$	−410	−503
ν_2	$C_\beta C_\beta$, $C_\alpha C_m$	−344	−297
ν_3	$C_\alpha C_m$, $C_\beta C_\beta$	−260	−390
ν_{11}	$C_\beta C_\beta$	−199	−406
ν_4	NC_α, $C_\alpha C_\beta$	−118[e]	−97

[a] Indicates major internal coordinate contribution to the potential energy distribution. [b] Slopes from best fit lines for the data in Figures 4 and 5. [c] Slopes calculated from the geometric model by bond length scaling of the empirical force constants (Figures 4 and 5). [d] Slopes calculated with QCFF/PI program (Figure 6). [e] Observed slope is −256 cm^{-1}/Å if $SnTPP(Cl)_2$ is omitted.

exception for each porphyrin. Systematic deviations of the data from the predicted lines are seen in several cases, however. For TPP, ν_2 and ν_3 are accurately calculated, and ν_{19} is fairly close to the predicted line, but ν_{10}, ν_{11}, ν_3, and ν_4 all show significant

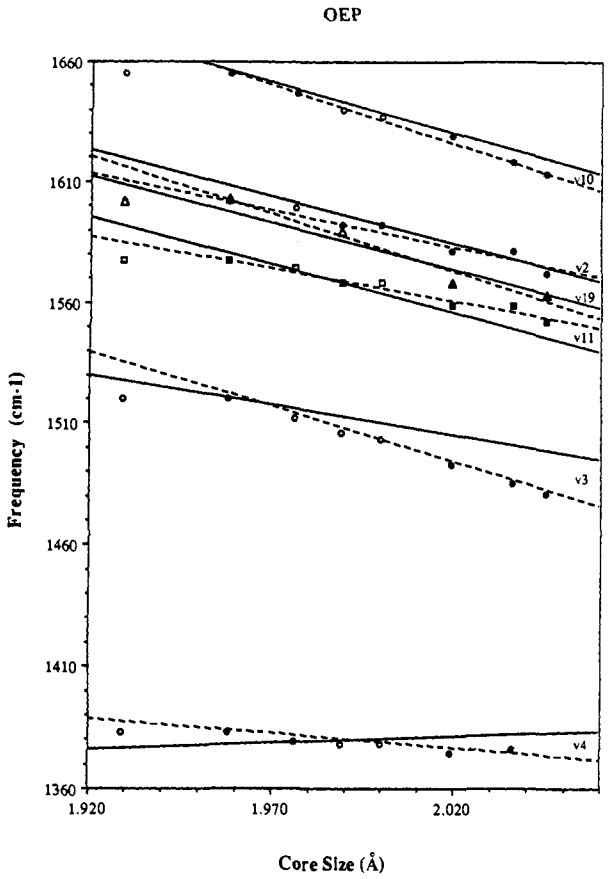

Figure 5. As Figure 4, but for OEP.

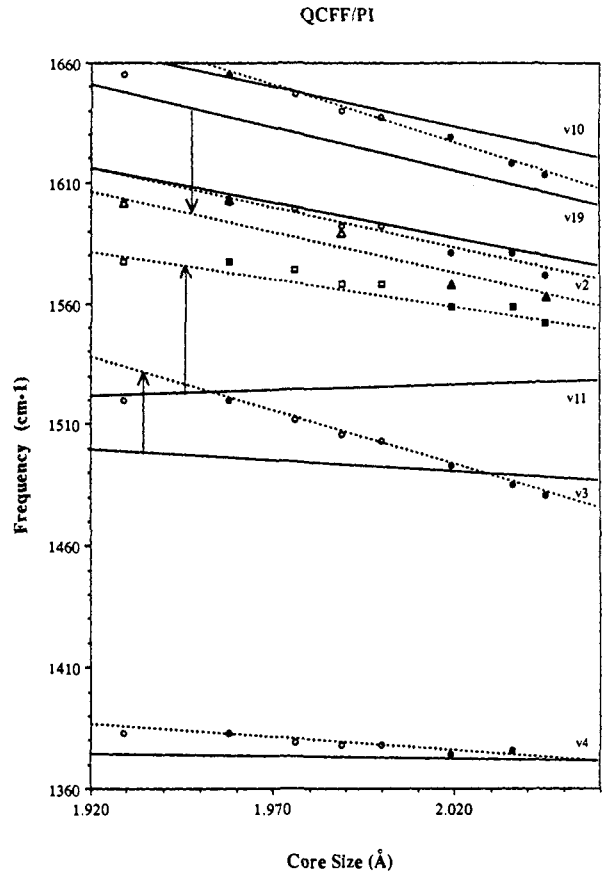

Figure 6. Core size dependence for OEP as calculated by QCFF/Pi (solid lines). The dotted lines are empirical best fit lines. Arrows connect the corresponding lines which are in substantial disagreement. Symbols as in Figure 4.

deviations. The agreement is better for OEP; only ν_3 and ν_4 show significant deviation from the predicted lines.

ν_4, the out-of-phase stretch of the $C_\alpha N$ and $C_\alpha C_\beta$ pyrrole bonds (half ring stretching),[2,3] is only weakly dependent on core size, and it seems to be affected by electronic factors that are not fully reflected in the bond distances. This mode responds to the oxidation state of iron porphyrin complexes in a manner which is not related to the core size.[8] The remaining modes have major contributions from $C_\alpha C_m$ and $C_\beta C_\beta$ stretching in various proportions. The deviant slopes may be partly related to the large amount of scatter in the $C_\beta C_\beta$ correlation with core size (Figure 2), which makes this part of the geometric model rather uncertain. Any change in the $C_\beta C_\beta$ dependence to improve the fit to ν_{11} or ν_3, however, would necessarily worsen the fit for other, well-calculated modes. A more complex variation of the force field than simple scaling of the principal stretching force constants is therefore probably required for accurate fitting. We did try one modification by allowing the stretch–stretch interaction constants to scale with the geometric mean of the stretching constants themselves. Although the calculated slopes changed slightly, the overall fit to the data did not improve.

2. QCFF/Pi Calculation. QCFF/Pi is a semiempirical electronic structure program, designed to calculate structures and vibrational frequencies efficiently, which is based on a PPP-level treatment of the electronic structure.[12] Its application to porphyrins was introduced by Warshel,[9] and Bocian and co-workers[26] have refined the parameters to permit more accurate calculation of porphyrin normal modes. We have used this version of the program to test its ability to model the core size effect, using planar NiOEP with point mass ethyl substituents and a point charge Ni(II) ion. The core size was varied by changing the Ni–N bond length parameter, b_0.[25] In Figure 2, we plot the calculated variations in the skeletal bond lengths with core size as dashed lines. The agreement with experiment is reasonably good except for $C_\beta C_\beta$, which is incorrectly calculated to shorten with increasing core size. The $C_\alpha C_m$ and $C_\alpha C_m C_\alpha$ correlations have the correct slopes, but are somewhat displaced in the magnitude of the bond distances from the OEP data, while the $C_\alpha N$ and $C_\alpha C_\beta$ slopes have the correct sign but are larger and smaller, respectively, than the experimental slopes.

Figure 6 shows the QCFF/Pi calculated frequencies versus core size as solid lines. The ν_{10} and ν_2 lines agree quite well with the experimental data for NiOEP, and the ν_{19} line has about the right slope but is displaced roughly 40 cm^{-1} from the experimental line. These modes all have mainly $C_\alpha C_m$ character. The ν_{11} and ν_3 calculations, however, disagree badly with the experiment, reflecting the incorrect prediction of the $C_\beta C_\beta$ length dependence. Thus, the semiempirical parameterization of QCFF/Pi captures only partially the electronic structure changes associated with core expansion.

B. Ruffling and Doming. While core size may serve satisfactorily to predict the skeletal mode frequencies of planar porphyrins, additional parameters may be needed when the skeleton is not planar. As noted above, the scatter in the core-size correlations is not significantly increased by the inclusion of complexes which are expected to be ruffled or domed when the data are plotted globally, as in Figures 2–6, but closer comparisons yield discrepancies which are attributable to skeletal distortions. The clearest example is provided by NiOEP, which crystallizes in both planar[27] and ruffled forms,[17,28] depending on solvent and tem-

(26) Boldt, N. J.; Donohoe, R. J.; Birge, R. R.; Bocain, D. F. *J. Am. Chem. Soc.* **1987**, *109*, 2284.

(27) Cullen, D. L.; Meyer, E. F. *J. Am. Chem. Soc.* **1974**, *96*, 2095.
(28) Brennan, T. D.; Scheidt, W. R.; Shelnutt, J. A. *J. Am. Chem. Soc.* **1988**, *110*, 3919.
(29) Li, X. Y.; Czernuszewicz, R. S.; Kincaid, J. R.; Spiro, T. G. *J. Am. Chem. Soc.* **1989**, *111*, 7012.
(30) Bangcharoenpaurpong, O.; Schomacker, K. T.; Champion, P. M. *J. Am. Chem. Soc.* **1984**, *106*, 5688.
(31) Scheidt, W. R.; Lee, Y. J.; Hatano, K. *J. Am. Chem. Soc.* **1984**, *106*, 3191.

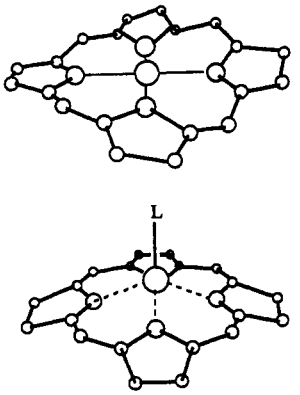

Figure 7. Representation of ruffling (top) and doming (bottom) of the porphyrin skeleton.

perature.[28] In the ruffled form (Figure 7), the pyrrole rings swivel about the Ni–N bonds, and the methine C_α atoms move alternately up and down with respect to the mean plane. This motion permits the core to contract, in order to accommodate the small low-spin Ni(II) ion. The Ni–N distance is 1.96 Å in the planar form, but 1.93 Å in the ruffled form. Despite this contraction, the skeletal mode frequencies are all *lower* in ruffled than in planar NiOEP,[4,10b,13] contrary to expectation based on the core size correlations.

Doming often occurs in 5-coordinate complexes,[15] when the central metal moves out of the porphyrin ring toward the fifth ligand (Figure 7). The extent to which the pyrrole rings follow this motion by tilting in the same direction varies from case to case. Often the tilting is negligible (these are the complexes labeled MOOP above) but sometimes the displacement of the average N plane from the average porphyrin plane can reach ca. 0.15 Å. There is no example of a complex occurring in both planar and domed polymorphs, but deviations from core size correlations have been noted for some domed porphyrins, especially involving Mn(II), Fe(II), and Co(II).[5]

1. Kinematics. In order to investigate the kinematic effects of out-of-plane distortions of the skeleton, we calculated the frequency differences for NiOEP in planar and ruffled or domed conformations. The structural parameters for planar and ruffled NiOEP were used directly, while for a hypothetical domed NiOEP, the bond distances were those of planar NiOEP, but the metal was displaced 0.42 Å out of the porphyrin plane in order to produce a displacement of the average nitrogen and carbon planes (P_N–P_C) of 0.13 Å, as observed in (2-MeImH)Fe^{II}TPP.[49] (The crystal structure of this compound is actually irregular, with one pyrrole tilted strongly and the other three very little, presumably due to packing effects. A more regular structure is expected in solution.) As pointed out by Hoard,[15] the pyrrole rings can be tilted moderately with no required change in any of the bond distances. The in-plane NiOEP force field[3] was held constant in these calculations, but the out-of-plane force field was added,[29] since some interaction of in- and out-of-plane modes becomes allowed in the ruffled and domed structures. Actually, this refinement made no difference to the high-frequency skeletal modes under consideration in this study, since the out-of-plane modes are all at much lower frequency, but it did influence modes below 850 cm^{-1}. These modes are left for discussion elsewhere.

Table V. Calculated Kinematic Effects of NiOEP Core Distortion[a]

mode	contribution[b]	planar	Δruffling[c]	Δdoming[c]
ν_{10}	$C_\alpha C_m$	1661	−14	−14
ν_2	$C_\beta C_\beta$, $C_\alpha C_m$	1607	+1	−4
ν_{19}	$C_\alpha C_m$	1607	−16	−17
ν_{11}	$C_\beta C_\beta$	1579	+1	−1
ν_3	$C_\alpha C_m$, $C_\beta C_\beta$	1523	+8	+4
ν_{28}	$C_\alpha C_m$, NC_α	1485	+4	+8
ν_{29}	$C_\alpha C_\beta$	1408	+5	−3
ν_{20}	NC_α, $C_\alpha C_\beta$	1393	+1	+12
ν_4	NC_α, $C_\alpha C_\beta$	1383	−9	−4

[a] All bond lengths were held at NiOEP planar values (ref 26). For the ruffled structure, the dihedrals from the NiOEP ruffled form were used (ref 17). The domed structure was generated assuming rigidly planar pyrrole rings which are tilted 20° out of the mean porphyrin plane, causing descending planes of atoms: metal, N, C_α, C_m, C_β. [b] Main internal coordinate contribution to the mode, as determined in ref 3. [c] Frequency shifts upon ruffling or doming, relative to the planar value.

The calculated skeletal mode differences due to the out-of-plane distortions are listed in Table V. Significant shifts are predicted for several modes. Interestingly, 14–17 cm^{-1} downshifts are predicted for ν_{10} and ν_{19} for both doming and ruffling. These modes both involve out-of-phase stretching of the two $C_\alpha C_m$ bonds joined at each C_m bridge.[3] The effect of either swiveling or tilting the pyrrole rings, in the ruffled or domed structure, is to tip the methine bridges out of the porphyrin plane. In this geometry, the C_m atoms can more easily move tangentially to the porphyrin ring, a motion involving the out-of-phase stretching of the $C_\alpha C_m$ bonds.

In Table VI, we gather the observed deviations[5] from the experimental core size plots for 5-coordinate complexes of Fe(II), Mn(II), and Co(II) with TPP and protoporphyrin (PP). All these metals give ν_{19} depressions which are in quite good agreement with the kinematic prediction, but ν_{10} shows an irregular pattern. For most of the complexes, ν_2, ν_3, and ν_{11} are fairly insensitive to doming, as expected, but there are outlying points for Mn^{II}PP (+14 cm^{-1} for ν_2) and Co^{II}PP (−10 cm^{-1} for ν_{11}). Thus, the data are in only partial agreement with the kinematics of doming. It is not immediately clear whether the discrepancies represent unaccounted electronic or geometric effects or lingering difficulties in the band assignments. Some of the bands are weak or poorly resolved in the available RR spectra[5] and may not be correctly assigned. In addition, we note that the actual degree of doming in the listed complexes is uncertain. The available crystal structures are (2-MeImH)Fe^{II}TPP,[49] (1-MeIm)Co^{II}OEP,[40] and (2MeIm)Mn^{II}TPP.[56] The first two of these show significant net

(32) Little, R. G.; Ibers, J. A. *J. Am. Chem. Soc.* **1974**, *96*, 4440.
(33) Scheidt, W. R.; Geiger, D. K.; Lee, Y. J.; Reed, C. A.; Lang, G. *J. Am. Chem. Soc.* **1985**, *107*, 3693.
(34) Molinaro, F. S.; Ibers, J. A. *Inorg. Chem.* **1976**, *15*, 2278.
(35) Scheidt, W. R.; Lee, Y. J.; Geiger, D. K.; Taylor, K.; Hatano, K. *J. Am. Chem. Soc.* **1982**, *104*, 3367.
(36) Cullen, D. L.; Meyer, E. F., Jr. *Acta Crystallogr.* **1973**, *B29*, 2507.
(37) Cullen, D. L.; Meyer, E. F.; Smith, K. M. *Inorg. Chem.* **1977**, *16*, 1179.
(38) Fleisher, E. B.; Miller, C. K.; Webb, L. E. *J. Am. Chem. Soc.* **1964**, *86*, 2342.
(39) Collman, J. P.; Hoard, J. L.; Kim, N.; Lang, G.; Reed, C. A. *J. Am. Chem. Soc.* **1975**, *97*, 2676.
(40) Scheidt, W. R. *J. Am. Chem. Soc.* **1974**, *96*, 90.
(41) Scheidt, W. R.; Cunningham, J. A.; Hoard, J. L. *J. Am. Chem. Soc.* **1973**, *95*, 8289.
(42) Scheidt, W. R. *J. Am. Chem. Soc.* **1974**, *96*, 84.
(43) Collins, D. M.; Countryman, R.; Hoard, J. L. *J. Am. Chem. Soc.* **1972**, *94*, 2066.
(44) Hoard, J. L. In *Porphyrins and Metalloporphyrins*; Smith, K. M., Ed.; Elsevier: New York, 1975; p 317ff.
(45) Li, N.; Coppens, P.; Landrum, J. *Inorg. Chem.* **1988**, *27*, 482.
(46) Radonovich, L. J.; Bloom, A.; Hoard, J. L. *J. Am. Chem. Soc.* **1972**, *94*, 2073.
(47) Hoffman, A. B.; Collins, D. M.; Day, V. W.; Fleischer, E. B.; Srivastava, T. S. *J. Am. Chem. Soc.* **1972**, *94*, 3620.
(48) Scheidt, W. R.; Kastner, M. E.; Hatano, K. *Inorg. Chem.* **1978**, *17*, 706.
(49) Hoard, J. L.; Scheidt, W. R. *Proc. Natl. Acad. Sci. U.S.A.* **1973**, *70*, 3919.
(50) Collins, D. M.; Scheidt, W. R.; Hoard, J. L. *J. Am. Chem. Soc.* **1972**, *94*, 6689.
(51) Czernuszewicz, R. S.; Macor, K. A.; Li, X. Y.; Kincaid, J. R.; Spiro, T. G. *J. Am. Chem. Soc.* **1989**, *111*, 3860.
(52) Madura, P.; Scheidt, W. R. *Inorg. Chem.* **1976**, *15*, 3182.
(53) Mashiko, T.; Kastner, M. E.; Spartalian, K.; Scheidt, W. R.; Reed, C. A. *J. Am. Chem. Soc.* **1978**, *100*, 6354.
(54) Kirner, J. F.; Garofollow, J.; Scheidt, W. R. *Inorg. Nucl. Chem. Lett.* **1975**, *11*, 107.
(55) Hoard, J. L.; Cohen, G. H.; Glick, M. D. *J. Am. Chem. Soc.* **1967**, *89*, 1992.
(56) Gonzalez, B.; Kouba, J.; Yee, S.; Reed, C. A.; Kirner, J. F.; Scheidt, W. R. *J. Am. Chem. Soc.* **1975**, *97*, 3247.

Table VI. Core Size Deviations[a] for 5-Coordinate Low Valent Complexes

	(2MeIm)Fe^{II}TPP	(2MeIm)Fe^{II}PPIX	(2MeIm)Mn^{II}TPP	(2MeIm)Mn^{II}PPIX	(2MeIm)Co^{II}PPIX
ν_2	0	0	0	+14	0
ν_3	−8	−6	0	−5	0
ν_4	−15	−13	−13	−10	−9
ν_{10}	NR[b]	0	+23	0	−13
ν_{11}	NR	0	0	0	−10
ν_{19}	NR	−12	NR	−15	−22

[a] Frequency shifts from ref 5. [b] NR, not reported.

Table VII. NiOEP Ruffled–Planar Frequency Differences (cm^{-1})

				calculated				
	experimental values[a]			kinematics[b]			scaled[c]	
mode	planar	ruffled	Δ[d]	planar	ruffled	Δ	ruffled	Δ
ν_{10}	1661	1640	−21	1658	1644	−14	1631	−27
ν_2	1607	1595	−12	1604	1605	+1	1573	−31
ν_{19}	1607	1586	−21	1601	1585	−16	1577	−24
ν_{11}	1579	1571	−8	1578	1579	+1	1532	−46
ν_3	1523	1513	−10	1517	1525	+8	1500	−17
ν_{28}	1485	1476	−9	1486	1490	+4	1487	+1
ν_{29}	1408	1405	−3	1400	1405	+5	1399	−1
ν_{20}	1393	1391	−2	1401	1402	+1	1398	−3
ν_4	1383	1383	0	1380	1371	−9	1370	−10

[a] Frequencies from crystalline RR spectra (ref 13). [b] No change in force field from ref 3 (see Table V). [c] Force constants scaled to bond distance changes in ruffled form. [d] Δ = planar frequency minus ruffled frequency.

doming, P_N–P_C = 0.15 and 0.16 Å (although the Fe(II) structure is irregular, as noted above), but the last complex has P_N–P_C of only 0.04 Å; the Mn(II) structure, however, actually shows a *saddle* structure with a significant average tilt of the pyrrole rings. The relationship of the solution structures to the crystal structures is difficult to judge because of the likelihood that packing forces influence the degree of pyrrole tilting.

However, ν_4, which is normally the strongest band in Soret-excited RR spectra, is reliably assigned, and its consistently large frequency depression points to an electronic effect, probably associated with the low-valent character of the metal ions in this group of complexes. The likeliest mechanism is interaction of the d_z^2 electrons with the highest (or next-highest) filled porphyrin π orbital, a_{2u}. This interaction becomes allowed in the C_{4v} symmetry of the 5-coordinate complexes, both orbitals becoming a_1 in character. The d_z^2 electrons are concentrated on the side of metal ion away from the fifth ligand, i.e. directly in the porphyrin cavity.

This mechanism for ν_4 reduction (which has also been invoked to account for variations in the Fe–histidine stretching frequency in hemoglobin[30]) is not linked to doming per se, but rather to five-coordination. It should be most effective with low-valent metal ions, whose d_z^2 electrons would extend farther and interact more strongly with porphyrin electrons. Consistent with this view, the five-coordinate complexes of higher valent metal ions, e.g. Fe(III), Mn(III),[5] or V(IV),[59] do not show negative deviations of ν_4 from the core-size plots. In addition, the effect should increase with the donor strength of the axial ligand, which interacts directly with the d_z^2 orbital. Indeed, very large depressions of ν_4 are seen for Fe(II) protoporphyrin when the axial ligand is thiolate, either in cytochromes P_{450}[61,62] or in a model complex.[63]

2. Bond Length Scaling for NiOEP. In the case of ruffling, data are available for crystalline samples of ruffled[17,28] and planar[27] forms of the same compound NiOEP and are listed in Table VII.

Table VIII. Experimental Bond Lengths[a] for NiOEP

bond	triclinic A	triclinic B	triclinic B′	triclinic$_{av}$[b]	tetragonal
NiN	1.958 (2)	1.946 (4)	1.958 (4)	1.955	1.929 (3)
$C_\alpha N$	1.376 (6)	1.392 (1)	1.379 (10)	1.389	1.386 (2)
$C_\alpha C_m$	1.371 (4)	1.362 (10)	1.365 (12)	1.368	1.372 (1)
$C_\alpha C_\beta$	1.443 (3)	1.439 (14)	1.450 (6)	1.444	1.449 (5)
$C_\beta C_\beta$	1.346 (2)	1.333 (8)	1.330 (8)	1.341	1.362 (5)

[a] All lengths in Å. Triclinic A values from ref 26, B from the two indepe nt molecules per unit cell in ref 27, and tetragonal from ref 17. [b] rage weighted by the inverse of the standard deviation (in parentheses) in the individual distances.

Downshifts are seen for ν_{10} and ν_{19}, and are somewhat larger than the kinematic prediction; there are several other downshifts which are in disagreement with the kinematic calculation. The disagreement implies electronic effects associated with the ruffling, and we looked for evidence of these effects in the ring bond lengths, listed in Table VIII. Planar NiOEP is found in two crystal forms, A and B, depending on solvent and crystallization conditions.[27] In form B, there are two independent NiOEP molecules in the unit cell. Consequently, there are three independently determined structures of planar NiOEP.[26,27] As can be seen in Table VIII, there is appreciable scatter in the bond lengths, as well as their estimated uncertainties, even for the two molecules in the same unit cell. These differences are unlikely to be real because they imply an appreciable spread of frequencies for the skeletal modes in vibrational spectra of crystalline samples of planar NiOEP. These samples are usually mixtures of forms A and B, and doubling is seen for some of the low-frequency RR bands which involve motions of the substituents (because of different relative orientations of the ethyl groups in the two forms).[29] The high-frequency skeletal modes, however, are seen as single bands of normal widths. Using difference techniques, Shelnutt and co-workers found a 2.5-cm^{-1} difference in the ν_4 frequency between form A and form B, possibly because of different stacking interactions.[28] A much larger difference (tens of cm^{-1}) would have been expected if the range of $C_\alpha N$ distances were actually as wide as reported, 0.016 Å. In fact, this range is encompassed by the sum of the standard deviations and is therefore not experimentally significant.

In order to obtain representative bond lengths for planar NiOEP, we averaged the three structures, weighting each bond length by the inverse of the stated uncertainty (standard deviations). These average values are also given in Table VIII. When they are compared to the bond lengths for the one ruffled NiOEP structure, it can be seen that the differences are quite small, except for the $C_\beta C_\beta$ bonds, which are nearly 0.02 Å longer in the ruffled structure. This lengthening might account for the frequency lowering of ν_2, ν_3, and ν_{11}, which have large $C_\beta C_\beta$ stretching contributions. To test this idea, we applied force constant scaling to the calculation of the ruffled NiOEP frequencies, using the averaged planar bond lengths as the reference distances. The resulting frequency changes, listed in Table VII, are in the right direction but are too large. In particular, ν_{11}, which is nearly pure $C_\beta C_\beta$ stretching in character, is calculated to shift by −46 cm^{-1}, whereas the observed shift is only −8 cm^{-1}. In view of the scatter in the planar NiOEP bond distance determinations, we are inclined to attribute this overshoot to uncertainty in the ruffled NiOEP bond lengths. If several ruffled structures were available, it might be that scaling to the averaged distances would give a more reliable calculation. This experience suggests that calculation of porphyrin vibrational frequencies according to the details of any one crystal structure determination is unlikely to give accurate results, re-

(57) Ozaki, Y.; Iriyama, K.; Ogoshi, H.; Kitagawa, T. *J. Am. Chem. Soc.* **1987**, *109*, 5583.
(58) Ozaki, Y.; Iriyama, K.; Ogoshi, H.; Kitagawa, T. *J. Phys. Chem.* **1986**, *90*, 6195.
(59) Su, Y. O.; Czernuszewicz, R. S.; Miller, L. A.; Spiro, T. G. *J. Am. Chem. Soc.* **1988**, *110*, 4150.
(60) Kim, D.; Su, Y. O.; Spiro, T. G. *Inorg. Chem.* **1986**, *25*, 3393.
(61) Champion, P. M.; Gonzales, I. C.; Wagner, G. C. *J. Am. Chem. Soc.* **1978**, *100*, 3743–3751.
(62) Ozaki, Y.; Kitagawa, T.; Kyogoku, Y.; Imai, Y.; Hashimoto-Yutsudo, C.; Sato, R. *Biochemistry* **1978**, *17*, 5826–5831.
(63) Anzenbacher, P.; Evangelista-Kirkup, R.; Schenkman, J.; Spiro, T. G. *Inorg. Chem.* **1989**, *28*, 4491–4495.

Table IX. Comparison of Observed and Predicted[a] Bond Lengths (Å) for Ruffled Porphyrins

	core	$C_\alpha N$	$C_\alpha C_m$	$C_\alpha C_\beta$	$C_\beta C_\beta$	ΔC_m[b]
NiOEP[17]						
expt	1.929	1.386	1.373	1.444	1.362	0.514
calc		1.385	1.371	1.442	1.341	
(3.5-Lut)CoTPPNO$_2$[44]						
expt	1.954	1.374	1.400	1.442	1.358	0.600
calc		1.389	1.385	1.437	1.345	
FeTPP[39]						
expt	1.972	1.382	1.392	1.436	1.353	0.400
calc		1.387	1.388	1.439	1.347	
Im$_2$FeTPPCl[43]						
expt	1.989	1.378	1.398	1.437	1.350	0.310
calc		1.385	1.390	1.440	1.350	
FeTPP(NCS)Py[35]						
expt	1.988	1.379	1.392	1.438	1.342	0.350
calc		1.385	1.390	1.440	1.350	

[a] Calculated from best-fit lines in Table II. [b] C_m average out-of-plane displacement in Å.

Table X. MNDO/3 Optimized Geometries for Zinc Porphine[a]

	D_{4h} (planar)	D_{2d} (ruffled)	C_{4v} (domed)
C_t–N, Å	2.069	2.038	2.070
NC_α, Å	1.393	1.391	1.393
$C_\alpha C_m$, Å	1.401	1.406	1.399
$C_\alpha C_\beta$, Å	1.469	1.469	1.469
$C_\beta C_\beta$, Å	1.371	1.373	1.369
$\Delta H_{formation}$, kcal/mol	194.9	211.1	209.5

[a] Point group constrained in the optimization. All bonds and angles were allowed to vary while the dihedrals were constrained as described in the text.

gardless of the physical adequacy of the model used.

3. MNDO/3 Calculation. Hoard[15] has noted that it should be possible to ruffle porphyrins with minimal changes in bond lengths, and we therefore wondered whether the substantial lengthening of $C_\beta C_\beta$ upon ruffling was peculiar to NiOEP. In Table IX, bond distances for several ruffled porphyrins are compared with the distances calculated on the basis of the expected core-size dependencies (Figure 2). Appreciably longer than expected $C_\beta C_\beta$ bonds are seen for NiOEP (0.021 Å) and, to a lesser extent (3,5-lutidine)(NO_2)Co^{III}TPP (0.013 Å).[44] These are the complexes with the smallest cores (1.93, 1.95 Å) and the largest extent of ruffling, with 0.51 and 0.60 Å displacement of the C_m atoms from the mean plane (ΔC_m). The remaining three complexes have larger cores, 1.97–1.99 Å, less ruffling (ΔC_m = 0.31–0.40 Å), and small deviations (<0.009 Å) of $C_\beta C_\beta$ from the expected length. We tentatively conclude that the $C_\beta C_\beta$ lengthening is associated with small cores, or with some other electronic influence on Ni(II) and Co(III).

To test the effect of imposing ruffling by a different mechanism, we carried out a MNDO/3 calculation[18] on an artificially ruffled porphyrin. This semiempirical electronic structure method gives reliable geometries for heterocycles, and in its current version[19] it is parametrized for Zn(II) ions. Consequently, we optimized the structure of zinc(II) porphine (all substituents are H), which converged to a planar structure with reasonable bond distances, all of which were a little long (Table X). Next, the structure was ruffled by constraining the dihedral angles so that the pyrrole rings swiveled by the angle observed in ruffled NiOEP.[17] When the geometry was reoptimized, the core size shrank by 0.03 Å, as expected, but the remaining bond distances were insignificantly different from those of the planar structure. A similar calculation was carried out on an artificially domed porphyrin, by constraining the z coordinates of all the atoms to the out-of-plane displacements seen for (2-MeIm)Fe^{II}TPP.[49] Again, there were negligible changes in the C–C and C–N bond lengths around the ring (Table X); the core size was also unaltered. (We note that these calculations could not be carried out with the QCFF/Pi program because it does not function properly with nonplanar π systems.)

The MNDO/3 calculations support Hoard's view[15] that it is possible to dome or ruffle the porphyrin ring to a modest extent without changing the ring bond lengths significantly. If these distortions are imposed externally, e.g. by packing forces in a crystal or by steric contacts in a protein, then it seems likely that the response of the vibrational frequencies should be predictable on purely kinematic grounds. The main effect of swiveling or tilting the pyrrole rings is expected to be a reduction in ν_{10} and ν_{19}, because of the required out-of-plane displacement of the C_m atoms. The actual frequency patterns displayed by domed and ruffled metalloporphyrins are more complex, because the geometric changes are convoluted with electronic effects associated with the metal ions.

Conclusions

The core-size dependence of metalloporphyrin skeletal mode frequencies is satisfactorily understood on the basis of the accompanying changes in the macrocycle bond lengths. As the core expands, so do all the outer ring bonds, $C_\alpha C_m$, $C_\alpha C_\beta$, and $C_\beta C_\beta$, while the $C_\alpha N$ bonds contract. The frequency correlations are calculated semiquantitatively by simply scaling the stretching force constants in the OEP or TPP force fields to the empirically determined bond distance/core-size correlations. These correlations apply about as well to nonplanar as to planar metalloporphyrins, although specific deviations for some nonplanar porphyrins are observed. The scatter in the data is significantly smaller for the vibrational frequencies obtained for complexes in solution than for the crystallographic bond distances, an effect attributed to the intrinsic uncertainty in the bond distance determinations.

Modest swiveling or tilting of the pyrrole rings to produce ruffled or domed porphyrins are not in themselves expected to influence the ring bond lengths. These distortions should have nonnegligible kinematic consequences for the skeletal mode frequencies, especially for the asymmetric $C_\alpha C_m$ stretches ν_{10} and ν_{19}, which are particularly sensitive to the out-of-plane displacement of the C_m atoms. Additional deviations from expectations based on core size seen for some ruffled or domed porphyrins are attributable to electronic effects.

These conclusions hold implications for the interpretation of heme protein resonance Raman spectra. The primary determinants of the skeletal mode frequencies are the oxidation state and the nature of the axial ligand(s), which together determine the core size. Deviations from the frequencies expected on the basis of core size occur when there are overriding electronic effects, which are again determined by the nature of the axial ligands. Large deviations are produced when strong donor ligands are bound in the Fe(II) state, resulting in back-donation of electrons to the porphyrin. All of these effects can be modeled by suitably chosen protein-free analogues. Additional frequency shifts are expected if the protein imposes a significant out-of-plane distortion on the porphyrin ring. The ν_{10} and ν_{19} frequencies are expected to be particularly sensitive to such distortion.

Acknowledgment. We thank Dr. Arieh Warshel for introducing us to QCFF/Pi; and Drs. David Bocian and Robert Donohoe for kindly providing their QCFF/Pi porphyrin parameters. This work was supported by DOE Grant FG02-81ER13876.

Registry No. NiOEP, 24803-99-4; TPP, 917-23-7.